Stem Cell Reports
Article

ISSCR

OPEN ACCESS

PTEN Mediates Activation of Core Clock Protein BMAL1 and Accumulation of Epidermal Stem Cells

Chiara Zagni,[1,5] Luciana O. Almeida,[1,5] Tarek Balan,[3] Marco T. Martins,[1] Luciana K. Rosselli-Murai,[1] Petros Papagerakis,[3,4] Rogerio M. Castilho,[1,2] and Cristiane H. Squarize[1,2,*]

[1]Laboratory of Epithelial Biology, Department of Periodontics and Oral Medicine, University of Michigan School of Dentistry, Ann Arbor, MI 48109-1078, USA
[2]Comprehensive Cancer Center, University of Michigan, Ann Arbor, MI 48109, USA
[3]OPD, University of Michigan School of Dentistry, Ann Arbor, MI 48109-1078, USA
[4]Center for Organogenesis, University of Michigan, Ann Arbor, MI 48109-2200, USA
[5]Co-first author
*Correspondence: csquariz@umich.edu
http://dx.doi.org/10.1016/j.stemcr.2017.05.006

SUMMARY

Tissue integrity requires constant maintenance of a quiescent, yet responsive, population of stem cells. In the skin, hair follicle stem cells (HFSCs) that reside within the bulge maintain tissue homeostasis in response to activating cues that occur with each new hair cycle or upon injury. We found that PTEN, a major regulator of the PI3K-AKT pathway, controlled HFSC number and size in the bulge and maintained genomically stable pluripotent cells. This regulatory function is central for HFSC quiescence, where PTEN-deficiency phenotype is in part regulated by BMAL1. Furthermore, *PTEN* ablation led to downregulation of BMI-1, a critical regulator of adult stem cell self-renewal, and elevated senescence, suggesting the presence of a protective system that prevents transformation. We found that short- and long-term PTEN depletion followed by activated BMAL1, a core clock protein, contributed to accumulation of HFSC.

INTRODUCTION

Epidermal stem cells (SCs) are localized in several well-defined cellular compartments with the best-studied being an anatomical area of the hair follicle (HF) known as "bulge" (Blanpain and Fuchs, 2009; Cotsarelis et al., 1990; Jaks et al., 2010). This unique anatomical site maintains SCs in a quiescent stage that is only interrupted by growth signals during new hair cycles or following tissue injury (Alonso and Fuchs, 2003; Morris et al., 2004). In either case, SCs exit the quiescent phase by migrating out of the bulge to initiate a new hair cycle or to repopulate a wounded site (Ito et al., 2007; Langton et al., 2008; Mascré et al., 2012). Therefore, tissue integrity requires the maintenance of a quiescent, yet responsive, population of SCs. New insights into the mechanism by which hair follicle stem cells (HFSCs) remain quiescent was revealed with the identification of NFATc1, a protein that controls cell-cycle progression (Horsley et al., 2008), the canonical BMP (bone morphogenetic protein) pathway, and, most recently, the core clock protein BMAL1 (Botchkarev and Sharov, 2004; Andl et al., 2004; Kobielak et al., 2003, 2007; Plikus et al., 2008; Lin et al., 2009; Janich et al., 2011). Tight control of SC quiescence ensures a sufficient supply of SCs for prolonged maintenance of tissue homeostasis and prevents tumor development by reducing DNA mutations caused by endogenous stress (Mohrin et al., 2010).

As powerful controllers of the cell cycle, tumor-suppressor genes may have an important role in the maintenance of SC quiescence (Sherr, 2004). Increasing evidence suggests that the PTEN (phosphatase and tensin homolog) tumor suppressor controls SC function in distinct tissue types, including the hematopoietic and mammary systems (Lee et al., 2010). Specifically, *Pten* controls hematopoietic SCs by preventing their release from the bone marrow niche, thereby reducing cell proliferation, self-renewal capacity, and the development of myeloproliferative disease (Zhang et al., 2006). In addition, reduced PTEN levels enrich normal and malignant human mammary SCs by activating the Wnt/β-catenin signaling pathway (Korkaya et al., 2009). Therefore, *PTEN* may control SC function in multiple organs and systems. We and others have previously reported that compromised *Pten* function contributes to epithelial transformation and tumor progression upon oncogenic stimulus (Squarize et al., 2008, 2013; Suzuki et al., 2003; Backman et al., 2004; Segrelles et al., 2014; White et al., 2014). These studies, using targeted deletion of *Pten* in the epidermis, suggest a broader regulatory role for PTEN in skin homeostasis and potentially in HFSC maintenance. Indeed, the role of PTEN in the biology of HFSCs remains poorly understood.

In this report, we investigated the role of *Pten* deficiency in HFSC maintenance and skin homeostasis. We found that monoallelic and biallelic excision of *Pten* led to delayed HF cycle. *Pten* deficiency induced uncontrolled accumulation of HFSC, as evidenced by an enlarged SC niche and increased number of SCs. We further observed that deregulation of *Pten* caused constitutive activation of the core circadian molecule BMAL1. Furthermore,

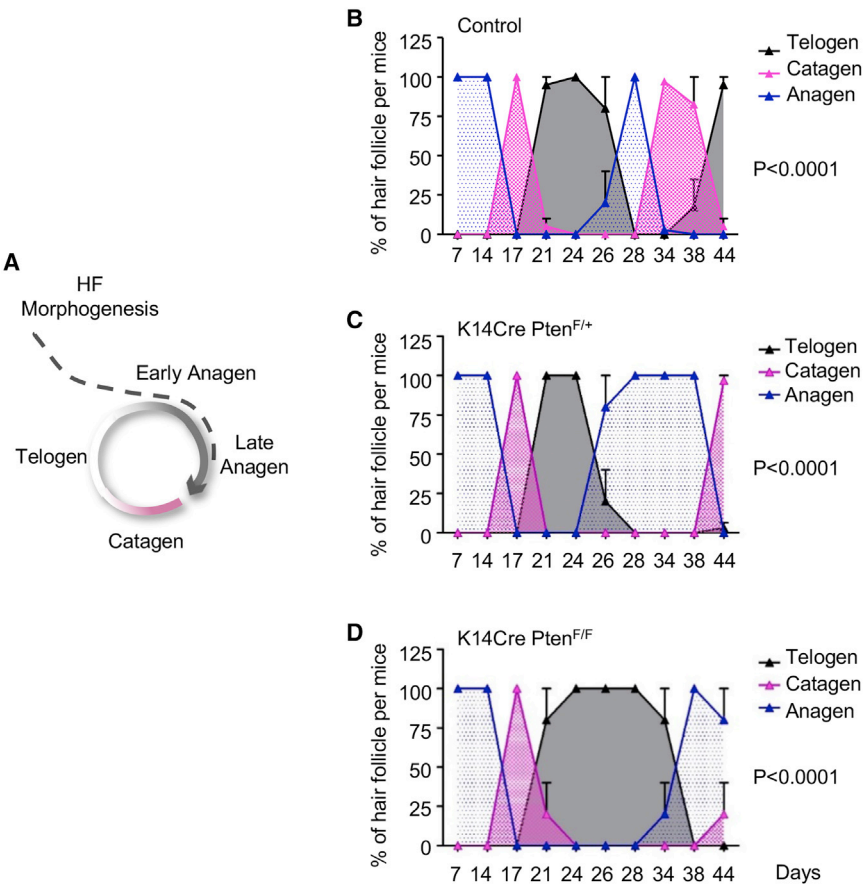

Figure 1. Lack of PTEN Disrupts the Synchronous Hair Follicle Cycle and Prolongs the Resting Phase

(A) Cyclic cycles during hair follicle (HF) morphogenesis comprise early and late anagen, catagen, and telogen phases.

(B–D) Graphic representation of the histological analyses of the synchronous hair cycle phases. As represented in control animals (B), the hair cycle follows a cyclic pattern in which the growth phase (anagen, blue), the involution phase (catagen, pink), and the resting phase (telogen, gray) are shown paired with the animals' age (days). (C) K14Cre-Pten$^{F/+}$ mice display a prolonged anagen in the second hair cycle. (D) K14Cre-Pten$^{F/F}$ mice have longer telogen phase. Data are presented as mean percentage ± SEM; n = 5 mice for each genotype.

loss-of-function assays performed in vivo revealed that expression of BMAL1 participates in the maintenance of the *Pten*-induced phenotype.

RESULTS

PTEN Regulates HF Cycling and Quiescence

To evaluate the biological effect of PTEN depletion in HSFCs and skin homeostasis in vivo, we generated epithelial-specific *Pten* conditional knockout mice by crossing mice harboring a floxed *Pten* allele (*Pten*^{tm1Hwu} or Pten$^{F/F}$) with mice that express the Cre recombinase driven by the K14 promoter (K14Cre) (Squarize et al., 2010). SCs at the bulge have alternating periods of dormancy and activation, which are reflected in the HF cycling (Fuchs, 2009; Nowak et al., 2008). The first two HF cycles are known to follow a fairly synchronous schedule in control mice (Paus et al., 1999a, 1999b). Each hair cycle comprises growth (anagen), regression (catagen), and quiescent (telogen) phases (Figure 1A), which are well characterized in wild-type mice (Figures 1B and S1A; Dry, 1926; Müller-Röver et al., 2001; Paus et al., 1999a, 1999b). In telogen, the SCs remain dormant (quiescent) as they wait for growth signals and progression to the anagen phase (Morris et al., 2004). First, we analyzed the abnormalities on the hair cycle and histomorphometry, which are strongly indicative of altered SC function. We found that single allele deletion of *Pten* (K14Cre-Pten$^{F/+}$) resulted in an extended anagen phase during the second hair cycle (Figures 1C and S1A). The alteration of the hair cycle upon PTEN deletion was enhanced with the biallelic excision of *Pten* (K14Cre-Pten$^{F/F}$), which resulted in extended telogen or quiescent phase (Figures 1D and S1A). These findings indicate that PTEN plays an important role in the hair cycle, which suggests a critical role in the control of SC function and quiescence. Additional histological analysis of the skin revealed that epithelial cell from K14Cre-Pten$^{F/F}$ mice displayed increased enlargement of the (interfollicular) basal cell layer, which is the cell layer harboring the interfollicular SCs, as well as increased skin keratinization (Figure S1B). Signs of cellular differentiation of HF cells (CK10 expression) were not different from the ones observed in control mice (Figure S1C). Nevertheless, the CK6 positive outer root sheath (ORS) cells were enlarged (Figure S1D), further suggesting the accumulation of SCs given that the HFSC

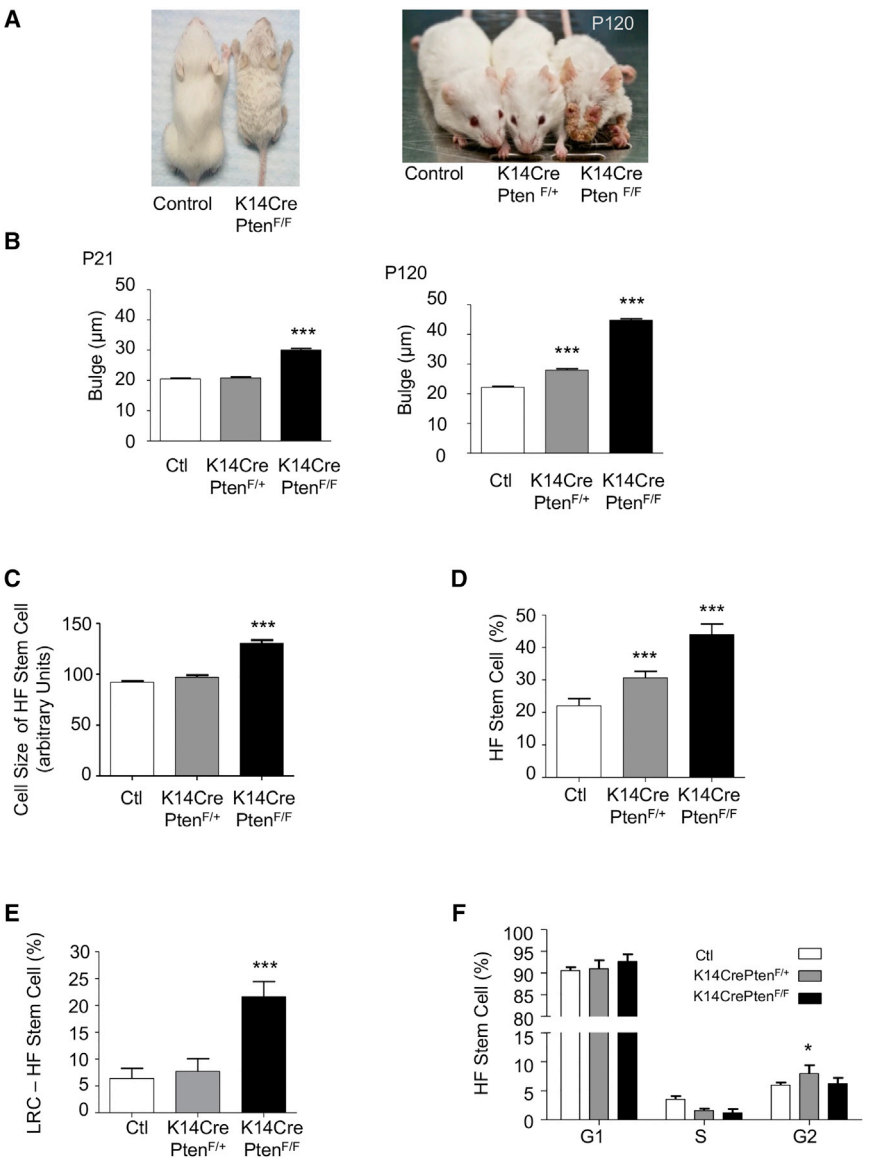

Figure 2. PTEN Ablation in the Epidermis Leads to Enlargement of the HFSC Niche and Accumulation of HFSCs

(A) Representative examples of K14Cre-Pten$^{F/F}$ mice displaying fur changes (disheveled appearance) from P12 through the remainder of their lives (n = 10 mice per genotype). As age progresses, K14Cre-Pten$^{F/F}$ mice display cutaneous changes, particularly in the vibrissae areas and eyelids as seen at P120.

(B) Bulge measurements for each phenotype (mean ± SEM; n = 20 for each genotype). ***p < 0.001.

(C) The cell size of HFSCs was calculated using FACS analysis (mean ± SEM, n = 10^4 cells per genotype). ***p < 0.001.

(D) Quantification of the number of HFSCs using FACS analysis. Note the increased number of stem cells in the K14Cre-Pten$^{F/+}$ and K14Cre-Pten$^{F/F}$ mice (mean percentage ± SEM, n = 10^4 cells per genotype). ***p < 0.001.

(E) Percentage of bromodeoxyuridine-label-retaining cells (LRC) in the hair follicle (HF) calculated by FACS analysis. Note that SC from K14Cre-Pten$^{F/F}$ mice had most LRC, indicating quiescent stem cells (mean percentage ± SEM, n = 10^4 cells per genotype). ***p < 0.001.

(F) FACS analysis of HFSCs showing the percentage of cells in G_1, S, and G_2 cell-cycle phases. Note that most stem cells are in G_1 arrest, especially the ones from K14Cre-Pten$^{F/F}$ mice. K14Cre-Pten$^{F/+}$ and K14Cre-Pten$^{F/F}$ displayed decreased DNA synthesis (S), although some stem cells from K14Cre-Pten$^{F/+}$ mice progressed to G_2 (mean percentage ± SEM, n = 10^4 cells per genotype). *p < 0.05.

niche is a specialized portion of the upper part of the ORS (Lavker et al., 2003). Independent of the PTEN status, the SCs were positive to the SC regulators β-catenin and pSMAD (Figures S1E and S1F). Altogether, our findings corroborate with the emerging concept that PTEN is involved in the SC function and hair cycle.

PTEN Deficiency Induces Expansion of the SC Niche and Increased Number of Quiescent SCs

We next analyzed the impact of *Pten* deficiency on skin homeostasis. Gene excision using the K14Cre-promoter in the follicular and interfollicular skin compartments that comprise the SC niche is well established (Nowak et al., 2008; Castilho et al., 2007; Merrill et al., 2001). To ensure the specificity of our findings, we used fluorescence-activated cell sorting (FACS) to identify the HFSCs (CD34$^+$α6-positive cells) (Trempus et al., 2003; Blanpain et al., 2004). Although newborn K14Cre-Pten$^{F/F}$ mice were mostly indistinguishable from control mice at birth, they had delayed hair coat growth, reduced body size, wrinkled flaky skin, and disheveled hair coat throughout their lifetimes (Figure 2A; postnatal day 21 [P21]). *Pten* mice also developed multiple epidermal alterations as they aged (Figure 2A; P120). Changes in the skin compartments were also accompanied by the enlargement of HFSC niche (Figure 2B; P21, p < 0.001). As the mice aged, bulges from K14Cre-Pten$^{F/+}$ (mean 27.94 ± 2.3 μm) and K14Cre-Pten$^{F/F}$ mice (mean 44.78 ± 2.27 μm) continued to expand

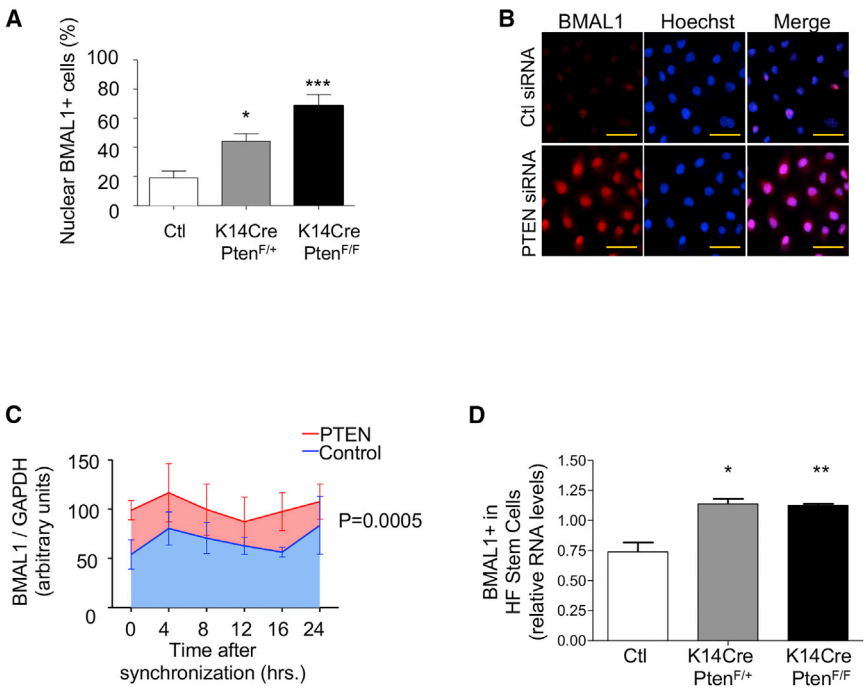

Figure 3. Loss of PTEN Induces Accumulation of Nuclear BMAL1 in the HFSCs

(A) Graphic shows the percentage of cells with active nuclear BMAL1 from K14Cre-Pten$^{F/+}$, K14Cre-Pten$^{F/F}$, and control mice (mean percentage ± SEM, n = 4 fields per three mice per genotype). *p < 0.05, ***p < 0.001.

(B) BMAL1 is activated and localized in the nucleus of PTEN-deficient human keratinocytes (NOK-SI cells). BMAL1 is activated in the nucleus of human keratinocytes following PTEN knockdown. Scale bars, 50 μm.

(C) Clock machinery follows a cyclic pattern. Densitometric analysis of protein bands on blots image of BMAL1 and GAPDH (control) from synchronized keratinocyte with siRNA control and siRNA for *PTEN*. Mean ± SEM, independent experiments in triplicates.

(D) Increased mRNA expression of *Bmail1* in HFSCs (isolated from mice using FACS sorting) (mean ± SEM; n = 6 per genotype). *p < 0.05; **p < 0.01.

(Figure 2B, p < 0.001). Collectively, these results show a continuous enlargement of the SC niche following PTEN excision. The niche expansion was a result of increasing SC number and size (Figures 2C and 2D). The SCs presenting PTEN biallelic excision became quiescent, as indicated by the increased numbers of label-retaining cells (LRCs) (Figure 2E) and delayed hair regrowth (Figures S2A and S2B, p < 0.01 and p < 0.001). The SCs from K14Cre-Pten$^{F/F}$ mice were mostly in G_1 arrest while SC with single allele deletion of *Pten* progressed to G_2 phase (Figure 2F).

Compromised *Pten* Function Results in the Accumulation of the Core Clock Protein BMAL1

Following the recent discovery that HFSC heterogeneity and quiescence may be affected by clock genes (Lin et al., 2009; Janich et al., 2011; Paus et al., 1999a, 1999b; Paus and Foitzik, 2004; Tanioka et al., 2009), we investigated whether the phenotype observed in *Pten*-deficient mice was associated with alterations in clock genes. We examined BMAL1 expression in the SCs and the follicular and interfollicular epidermis of *Pten* conditional knockout mice. Skin samples from control mice showed reduced nuclear localization of active BMAL1. K14Cre-Pten$^{F/+}$ and K14Cre-Pten$^{F/F}$ mice showed significant nuclear accumulation of BMAL1 (Figures 3A and S3A). To better characterize the *Pten* control on BMAL1, we used small interfering RNA (siRNA) technology to downregulate *PTEN* in human epithelial cells. Downregulation of *PTEN* resulted in nuclear accumulation of BMAL1 and increased levels of pAKT^{Ser473} (Figures 3B, S3B, and S3C; p < 0001). Notably, *PTEN* knockdown gene positively regulates BMAL1 expression in the epidermal cells, which maintained a cycling pattern (Figure 3C). Most importantly, *Bmal1* upregulation was confirmed in HFSCs of K14Cre-Pten$^{F/+}$ and K14Cre-Pten$^{F/F}$ mice (Figure 3D). We also analyzed whether upregulation of *Bmal1* affects the SCs. PER2 is a core negative transcriptional inhibitor of the circadian clock and controls BMAL1 and CLOCK (Fu et al., 2002). mPer2 knockout mice have constitutively active BMAL1 (Figure S3D). Depletion of Per2 from the epidermis resulted in the accumulation of HSFCs compared with control littermates (Figure S3E).

Pten-Deficient Mice Develop Small Wart-Like Lesion, i.e., Hamartoma, Characterized by Overexpression of BMAL1 and Activation of Cellular Senescence

Complete *Pten* ablation from the proliferative compartment of the epidermis resulted in increased wart formation on the face and limbs of mice (Figure 4A), in line with our previous report (Squarize et al., 2008). In particular, *Pten* was also associated with the development of progressive acanthosis of the epidermis (thickening of the skin) (Figure 4A) and the development of benign warts in aging mice (Figure 4B). Interestingly, benign warts (hamartomas) that originated on the skin of *Pten*-deficient mice were self-limited and the cells resembled the normal cellular component of the HF, including the sebaceous glands, ORS, and inner root sheath (Figures 4B and 4C).

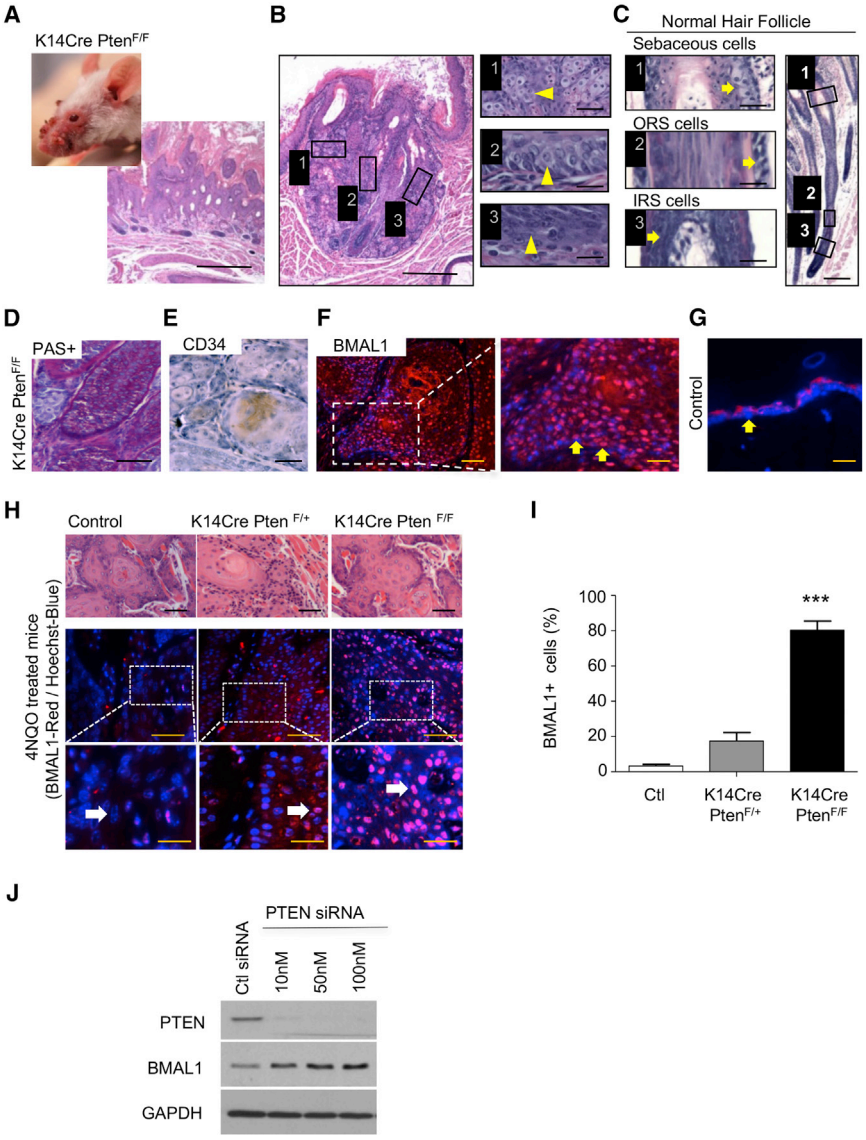

Figure 4. Sole Long-Term PTEN Depletion and Senescent Hamartomas

(A) Images of K14Cre-Pten$^{F/F}$ mice showing cutaneous warts on the face. H&E sections depicting epithelial acanthosis (larger spinous layer) and hyperkeratosis. Scale bar, 200 μm.

(B) Hamartomas are composed of cell types (yellow arrowheads) that closely resemble the internal structures of a normal hair follicle; yellow arrows, showing (1) sebaceous glands, (2) outer root sheath (ORS), and (3) inner root sheath (IRS). Scale bar, 200 μm; scale bars in insets, 25 μm.

(C) The normal hair follicle structures (from control mice) are composed of many epithelial layers and specialized cells including (1) sebaceous cells, (2) outer root sheath (ORS) cells, and (3) inner root sheath (IRS) cells that are also present in tumors (yellow arrows). Scale bar, 200 μm; scale bars in insets, 25 μm.

(D) Periodic acid-Schiff (PAS) staining depicting cells from hair follicle-derived ORS cells. Scale bar, 25 μm.

(E) Immunohistochemistry shows positive staining for the CD34 stem cell marker. Scale bar, 25 μm.

(F and G) Anti-BMAL1 staining of lesions from PTEN-deficient mice (F) showing numerous strong nuclear localizations (yellow arrows) compared with control epithelium (G). Scale bars, 100 μm; scale bar in inset, 25 μm.

(H–J) Chemically induced epithelial tumors with 4NQO (carcinomas) on PTEN-deficiency mice (H, I) and human samples (J) have increased expression of BMAL1. White arrows show nucleus in blue and BMAL1 in red. Scale bars in (H), 200 μm and (insets) 25 μm. Data in (I) represent mean percentage ± SEM, n = 4 per genotype; ***p < 0.001.

Remarkably, even after long-term follow-up, malignant transformation of epidermal cells was not detected in our PTEN-deficient mice. As seen in Figure S4, *Pten* disruption on the skin activates cellular senescence, a biological process that enables critical protection against malignant conversion. Senescence was identified by well-established hallmarks of cellular senescence (Castilho et al., 2009; Liu et al., 2007; Dimri et al., 1995), including endogenous β-galactosidase (SA-β-Gal) activity at pH 6, accumulation of nuclear γ-H2AX, and p16^{ink4} (Figures S4A–S4C). Additionally mice develop trichilemmomas, which are also seen in patients with PTEN deficiency (Squarize et al., 2008). These benign lesions of the HF are characterized by cells derived from the ORS and by positive periodic acid-Schiff staining (Figure 4D). Notably, trichilemmomas are highly enriched with cells that express the CD34 SC marker, as observed in the skin from our animal model (Figure 4E). Human trichilemmomas also express CD34 (Sanders and Carr, 2007). These results indicate that alterations derived following complete ablation of *PTEN* have many of the morphological characteristics and molecular signatures of HFs and their SCs. The lesions derived from K14Cre-Pten$^{F/F}$ mice retained high levels of BMAL1 (Figure 4F) compared with control littermates (Figure 4G),

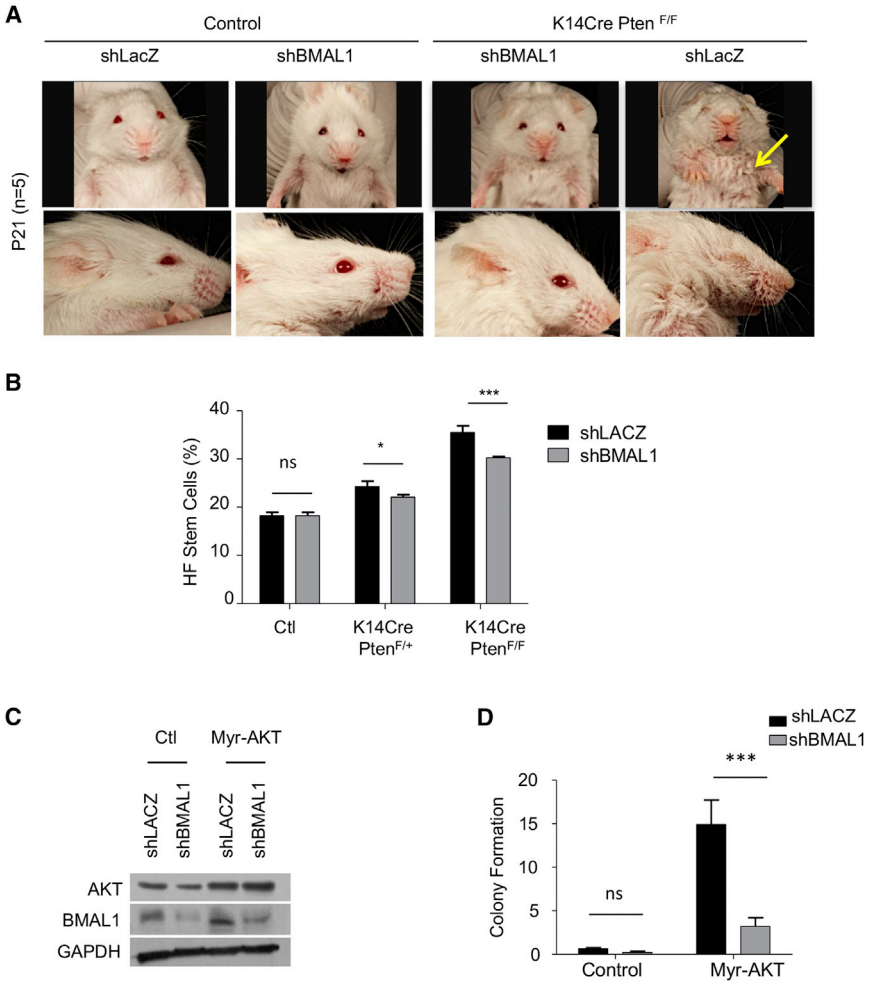

Figure 5. BMAL1 Ablation Reduces PTEN-Associated Stem Cell Accumulation

(A) Examples of control and PTEN-deficient mice after BMAL1 knockdown (Ad-shBmal1) or Ad-shLacZ. Note that K14CrePTEN mice displayed disheveled fur (yellow arrow). Rescue of the phenotype of K14CrePTEN mice with Ad-shBmal1 resembles controls animals (n = 5 mice per group).

(B) BMAL1 knockdown also reduced PTEN-driven stem cell accumulation (mean percentage ± SEM, n = 5 per genotype). *p < 0.05, ***p < 0.001.

(C) Immunoblot showing BMAL1 knockdown produced by Ad-shBMAL1 transduction.

(D) Graphic representation of colony formation assay depicting that BMAL1 knockdown decreases the number of individual colonies with AKT activation (Myr-AKT) (mean ± SEM, sextuplicates). ***p < 0.001.

suggesting that clock genes are consistently involved in the *PTEN*-driven phenotype. Interestingly, even after senescence is surpassed by chemical carcinogenesis (4-nitroquinoline 1-oxide [4NQO]), BMAL1 overexpression was found in PTEN-derived carcinomas (Figures 4H and 4I; Squarize et al., 2013), as well as in human carcinomas with PTEN knockdown (Figure 4J).

PTEN/AKT-Induced Accumulation of SCs Is Partially Regulated by BMAL1

We have shown that PTEN deletion in the skin triggers accumulation of SCs and activation of BMAL1. To test whether BMAL1 is actively involved in the accumulation of SCs upon PTEN excision, we deleted *Bmal1* in vivo using short hairpin (sh) technology (shBmal1 or shLacZ control, n = 5/group). Interestingly, we found that administration of shBMAL1 resulted in the partial rescue of the Pten-induced phenotype, including attenuation of the disheveled fur phenotype compared with control mice receiving shLacZ (Figure 5A). Furthermore, decreased Bmal1 expression reduced the accumulation of SCs in PTEN-deficient mice (Figure 5B). Because it is well known that the loss of PTEN activates the phosphatidylinositol 3-kinase/protein kinase B/mammalian target of rapamycin (PI3K/AKT/mTOR) pathway and that the phenotypic alterations driven by PTEN loss involve AKT activation (Sun et al., 1999; Squarize et al., 2008), we investigated whether BMAL1 knockdown would interfere with AKT-induced effects. Here we found that BMAL1 knockdown was able to interfere with the biological effects following AKT activation (Myr-AKT), which resulted in decreased numbers of colony formation (Figures 5C and 5D). Altogether, these results suggest that BMAL1 may participate in PTEN molecular signaling.

DISCUSSION

Molecular signals involved in the control of SCs are often associated with the PI3K pathway, which is activated in

neural, mammary, HF, and hematopoietic SCs (Korkaya et al., 2009; Kobielak et al., 2007; Groszer et al., 2006; Pietras et al., 2011; Polak and Buitenhuis, 2012; Segrelles et al., 2014). PI3K signaling is regulated by the *PTEN* tumor suppressor, a phosphatase that targets the second-messenger molecule phosphatidylinositol 3,4,5-trisphosphate and is an emerging regulator of normal SC function (Zhang et al., 2006; Fukuyama et al., 2006; Yilmaz et al., 2006). The *Pten*-deficient mouse phenotype, which includes striking alterations in the hair coat, suggested dysregulation of HFSC function. Indeed, under homeostatic conditions, deletion of *Pten* in the epidermis resulted in a progressive accumulation of SCs in the niche (bulge). The requirement for PTEN in HFSC homeostasis was further emphasized by the $CD34^{+}\alpha6$ cell accumulation following single and double allele deletion of *Pten*, indicating that *Pten* deficiency is sufficient to interfere with HFSC homeostasis. The accumulation of SCs in control mice occurs as age progresses (Doles et al., 2012), and this accumulation is increased by PTEN deletion.

Further characterization of the downstream molecular mechanism involved in the *Pten*-driven accumulation of HFSCs resulted in the identification of activation of the core circadian molecule BMAL1. BMAL1 regulates the timing of the HF cycle and promotes activation of HFSCs following external signals, such as transforming growth factor β and Wnt (Lin et al., 2009; Janich et al., 2011). Aligned with our results, in vivo studies on animals lacking BMAL1 in the epidermis generate epidermal SCs with reduced clonogenic potential, delayed anagen, and fewer proliferative cells, and therefore with constant proportion of bulge SCs in adulthood (Lin et al., 2009; Janich et al., 2011; Plikus et al., 2013). Similarly, constitutive activation of BMAL1 in the Per1/2 knockout mice resulted in more clonogenic epidermal SCs (Janich et al., 2011). These molecular changes affected hair growth (Plikus et al., 2013; Geyfman et al., 2012; Gaddameedhi et al., 2011; Mitra, 2011). Indeed after shaving, older adult PTEN mice displayed a halt in hair growth.

Loss of tumor-suppressor genes is involved in increased tumor predisposition in leukemogenesis and brain, prostate, intestinal, breast, and skin tumors (Squarize et al., 2008, 2013; Yan et al., 2002; Li et al., 2002; Fukuda et al., 2005; Guldberg et al., 1997; He et al., 2007; Ming et al., 2011). However, the biological features underlying such mechanisms are still poorly understood. Interestingly, K14Cre-$Pten^{F/F}$ mice did not spontaneously develop malignant tumors in the skin; on the contrary, we found hamartomas (benign lesions) characterized by the presence of well-differentiated HF cells and increased levels of the $p16^{ink4}$ senescence marker. Activation of cellular senescence often occurs during the development of benign lesions/tumors and restrains tumor size and malignant transformation (Dimri et al., 1995). Our findings are similar to those of White et al. (2014), who could not identify tumor formation upon short-term depletion of *Pten*. Although our promoter strategy (K14) differs from those used by White et al. (2014) (K15 and Lgr5), in both reports *Pten* deletion comprised the SC compartment of the epidermis. Interestingly, while we showed that the long-term accumulation of DNA damage preceded senescence and tumor formation in the presence of a carcinogen (4NQO), White et al. (2014) were able to induce tumor formation through the activation of Kras oncogene, a strategy to induce and expedite tumor formation. Of note, the development of malignant epidermal tumors was only observed upon the combined deletion of two tumor-suppressor genes (*Pten* and p53) along with constitutive activation of the Kras oncogene. It is also noteworthy that if a chemical carcinogen is applied, the resulting tumor with PTEN loss displays overexpresses BMAL1. This same correlation is seen in human tumors, and the BMAL1 expression is also dependent in PTEN and mTOR signaling (Matsumoto et al., 2017).

In humans, the autosomal dominant PTEN-deficient disorder Cowden's syndrome displays the development of multiple mucocutaneous hamartomas (Squarize et al., 2008). The mucocutaneous lesions in patients with Cowden's disease take years to develop (Hobert and Eng, 2009). In mouse models, the mucocutaneous lesions also have age-related penetrance (Squarize et al., 2008), which indicates that an accumulative effect of the PTEN deficiency is important for the phenotype development in vivo. Consistent with these clinical and experimental findings, short-term deletion of PTEN (e.g., over a period of 3–4 weeks) during adulthood is not enough to trigger hair cycle alterations and tumor development phenotype (White et al., 2014; Squarize et al., 2013; Chen et al., 2011; Kalaany and Sabatini, 2009), and cellular senescence usually occurs (White et al., 2014; Collado et al., 2005; Chen et al., 2005; Nardella et al., 2011).

Searching for a possible mechanism to explain the activation of cellular senescence, we found that silencing BMI-1 and the presence of $p16^{ink4}$ precede (and protect against) the development of skin tumors in K14Cre-$Pten^{F/F}$ mice. BMI-1 is a transcriptional repressor that is involved in cell-cycle arrest, SC longevity, and replicative senescence (Itahana et al., 2003; Lessard and Sauvageau, 2003; Park et al., 2004; Barker et al., 2008; Liu et al., 2009). Loss of BMI-1 leads to premature cellular senescence and increased $p16^{ink4}$ and $p19^{arf}$, proteins encoded by the *ink4a* gene (Jacobs et al., 1999a). In contrast, BMI-1 overexpression triggers an oncogenic effect mediated by $p16^{ink4}$ suppression and subsequent pRB and p53 signaling activation (Jacobs et al., 1999a, 1999b).

Following oncogene activation, such as *Ras*, cellular transformation results from Bmi-1 activation or $p16^{ink4}$ suppression (Kamijo et al., 1997; Serrano et al., 1996), suggesting a balance between Bmi-1 and $p16^{ink4}$ expression during the control or prevention of neoplastic occurrence.

In addition, our challenge was to identify and characterize the hierarchical interactions between PTEN and BMAL1. Evidence of this possible interplay of BMAL1 and PTEN deficiency came from the observation that *Bmal1* knockout mice have reduced the burden of squamous cell carcinoma and reduced $CD34^{+}\alpha6^{HI}$ (also referred as α6bright/$CD34^{+}$ tumor-initiating cells) (Janich et al., 2011). Furthermore, we challenged our *Pten*-deficient mice with the knockdown of BMAL1 before the development of the phenotype (day 3). We found that in vivo delivery of Ad-shBMAL1 was sufficient to rescue the skin phenotype, and the accumulation of HFSCs in both heterozygous and homozygous *Pten*-deficient mice. Interestingly, the foci formation driven by overexpression of the PI3K/AKT pathway was rescued upon downregulation of BMAL1. Our findings indicate that *Pten*-induced phenotype may be in part regulated by the clock core gene BMAL1 to induce accumulation of HFSC, which depicts a unique integration of PI3K and the clock gene signaling pathways during epidermal homeostasis.

EXPERIMENTAL PROCEDURES

Mice

All animal studies were carried out according to the University of Michigan approved protocols and in compliance with the Guide for the Care and Use of Laboratory Animals. Epithelial-specific *Pten* knockout mice were obtained by crossing $Pten^{F/F}$ mice (*Pten*^{tm1Hwu}) with K14Cre- (KRT14-cre) mice as described by Squarize et al. (2008). *mPer2* knockout mice (*Per2*^{tm1Drw}) were genotyped as previously described (Bae et al., 2001; Hoogerwerf et al., 2010). Mice were entrained to restricted 12-hr light/dark cycles. Where indicated, LRC was performed by injecting mice with bromodeoxyuridine (50 μg/g body weight) as described previously (Bickenbach and Chism, 1998; Braun and Watt, 2004). For further details see Supplemental Experimental Procedures.

FACS Analysis, Normal Keratinocyte Cell Line, and Immunohistochemistry/Immunofluorescence

SCs from the skin of 21-day-old and 17-week-old littermate mice were stained for CD34-FITC (BD Pharmingen, #553733) and CD49f-PE/Cye5 (BD Pharmingen, #551129) for FACS analysis as previously described (Castilho et al., 2009). Isotype controls were used as negative controls. HN13, NIH3T3, and NOK-SI cells were cultivated as described by Castilho et al. (2010). Immunohistochemistry or immunofluorescence was conducted with BMAL1 (Novus Bioscience, NB100-2288) overnight at 4°C (see Supplemental Experimental Procedures for details).

siRNA, SA-β-Gal, Immunoblotting, Adenoviruses, and Statistical Analysis

Cellular senescence was detected using an SA-β-Gal detection kit (Roche) at pH 6.0. Knockdown of PTEN or BMAL1 was achieved in NOK-SI and HN13 cells using siRNA. BMAl1 shRNA in vivo and in vitro experiments were conducted with Ad-shBmal1 or Ad-shLacZ-control, which was kindly provided by Dr. L. Yin (University of Michigan). Where indicated, Ad-shLacZ control or Ad-shBmal1 shRNA adenoviruses were injected into mice (age P3) subcutaneously at a dose of 1×10^{12} plaque-forming units (Zhang et al., 2014; Liu et al., 2007). The targeting sequence for mouse Bmal1 is 5′-CAT CGA TAT GAT AGA TAA CG-3′. All the adenoviruses were produced in 293AD packaging cells (Agilent) after Lipofectamine-mediated transfection, and concentrated after ultracentrifuge in cesium chloride gradient solutions. Mice were euthanized at P21, and SCs from skin were isolated and quantified by FACS analyses (UM Flow Cytometry Core). See Supplemental Experimental Procedures for additional details.

SUPPLEMENTAL INFORMATION

Supplemental Information includes Supplemental Experimental Procedures and four figures and can be found with this article online at http://dx.doi.org/10.1016/j.stemcr.2017.05.006.

AUTHOR CONTRIBUTIONS

C.Z., L.O.A., and R.M.C. designed and performed the assays; T.B. and P.P. contributed to mPER2 in vivo experiments; M.T.M. contributed to in vivo experiments; R.M.C. performed bioinformatics analyses; L.K.R.-M. performed BMI-1 and p16 experiments; R.M.C. and C.H.S. analyzed and interpreted the data, wrote the manuscript, and designed and supervised the study.

ACKNOWLEDGMENTS

We thank Drs. A.A. Dlugosz and G. Núnez for critically reviewing the manuscript. The work was partially funded by CNPq (246296/2012-7), UM faculty grant, and the Robert Wood Johnson Foundation (AMFDP- 72425), and NCI/NIH P30CA046592. We thank Dr. L. Yin and Dr. J.S. Gutking, who kindly provided the adenoviruses and Myr-AKT plasmids, and A. Robida and M. Savary for the FACS operation and cell-cycle analysis.

Received: December 22, 2014
Revised: May 2, 2017
Accepted: May 3, 2017
Published: June 8, 2017

REFERENCES

Alonso, L., and Fuchs, E. (2003). Stem cells in the skin: waste not, Wnt not. Genes Dev. *17*, 1189–1200.

Andl, T., Ahn, K., Kairo, A., Chu, E.Y., Wine-Lee, L., Reddy, S.T., Croft, N.J., Cebra-Thomas, J.A., Metzger, D., Chambon, P., et al. (2004). Epithelial Bmpr1a regulates differentiation and proliferation in postnatal hair follicles and is essential for tooth development. Development *131*, 2257–2268.

Backman, S.A., Ghazarian, D., So, K., Sanchez, O., Wagner, K.U., Hennighausen, L., Suzuki, A., Tsao, M.S., Chapman, W.B., Stambolic, V., and Mak, T.W. (2004). Early onset of neoplasia in the prostate and skin of mice with tissue-specific deletion of Pten. Proc. Natl. Acad. Sci. USA *101*, 1725–1730.

Bae, K., Jin, X., Maywood, E.S., Hastings, M.H., Reppert, S.M., and Weaver, D.R. (2001). Differential functions of mPer1, mPer2, and mPer3 in the SCN circadian clock. Neuron *30*, 525–536.

Barker, N., van de Wetering, M., and Clevers, H. (2008). The intestinal stem cell. Genes Dev. *22*, 1856–1864.

Bickenbach, J.R., and Chism, E. (1998). Selection and extended growth of murine epidermal stem cells in culture. Exp. Cell Res. *244*, 184–195.

Blanpain, C., and Fuchs, E. (2009). Epidermal homeostasis: a balancing act of stem cells in the skin. Nat. Rev. Mol. Cell Biol. *10*, 207–217.

Blanpain, C., Lowry, W.E., Geoghegan, A., Polak, L., and Fuchs, E. (2004). Self-renewal, multipotency, and the existence of two cell populations within an epithelial stem cell niche. Cell *118*, 635–648.

Botchkarev, V.A., and Sharov, A.A. (2004). BMP signaling in the control of skin development and hair follicle growth. Differentiation *72*, 512–526.

Braun, K.M., and Watt, F.M. (2004). Epidermal label-retaining cells: background and recent applications. J. Investig. Dermatol. Symp. Proc. *9*, 196–201.

Castilho, R.M., Squarize, C.H., Patel, V., Millar, S.E., Zheng, Y., Molinolo, A., and Gutkind, J.S. (2007). Requirement of Rac1 distinguishes follicular from interfollicular epithelial stem cells. Oncogene *26*, 5078–5085.

Castilho, R.M., Squarize, C.H., Chodosh, L.A., Williams, B.O., and Gutkind, J.S. (2009). mTOR mediates Wnt-induced epidermal stem cell exhaustion and aging. Cell Stem Cell *5*, 279–289.

Castilho, R.M., Squarize, C.H., Leelahavanichkul, K., Zheng, Y., Bugge, T., and Gutkind, J.S. (2010). Rac1 is required for epithelial stem cell function during dermal and oral mucosal wound healing but not for tissue homeostasis in mice. PLoS One *5*, e10503.

Chen, Z., Trotman, L.C., Shaffer, D., Lin, H.-K., Dotan, Z.A., Niki, M., Koutcher, J.A., Scher, H.I., Ludwig, T., Gerald, W., et al. (2005). Crucial role of p53-dependent cellular senescence in suppression of Pten-deficient tumorigenesis. Nature *436*, 725–730.

Chen, F., Li, Y., Wang, L., and Hu, L. (2011). Knockdown of BMI-1 causes cell-cycle arrest and derepresses p16INK4a, HOXA9 and HOXC13 mRNA expression in HeLa cells. Med. Oncol. *28*, 1201–1209.

Collado, M., Gil, J., Efeyan, A., Guerra, C., Schuhmacher, A.J., Barradas, M., Benguría, A., Zaballos, A., Flores, J.M., Barbacid, M., et al. (2005). Tumour biology: senescence in premalignant tumours. Nature *436*, 642.

Cotsarelis, G., Sun, T.T., and Lavker, R.M. (1990). Label-retaining cells reside in the bulge area of pilosebaceous unit: implications for follicular stem cells, hair cycle, and skin carcinogenesis. Cell *61*, 1329–1337.

Dimri, G.P., Lee, X., Basile, G., Acosta, M., Scott, G., Roskelley, C., Medrano, E.E., Linskens, M., Rubelj, I., and Pereira-Smith, O. (1995). A biomarker that identifies senescent human cells in culture and in aging skin in vivo. Proc. Natl. Acad. Sci. USA *92*, 9363–9367.

Doles, J., Storer, M., Cozzuto, L., Roma, G., and Keyes, W.M. (2012). Age-associated inflammation inhibits epidermal stem cell function. Genes Dev. *26*, 2144–2153.

Dry, F.W. (1926). The coat of the mouse (*Mus musculus*). J. Genet. *16*, 287–340.

Fuchs, E. (2009). The tortoise and the hair: slow-cycling cells in the stem cell race. Cell *137*, 811–819.

Fukuda, R., Hayashi, A., Utsunomiya, A., Nukada, Y., Fukui, R., Itoh, K., Tezuka, K., Ohashi, K., Mizuno, K., Sakamoto, M., et al. (2005). Alteration of phosphatidylinositol 3-kinase cascade in the multilobulated nuclear formation of adult T cell leukemia/lymphoma (ATLL). Proc. Natl. Acad. Sci. USA *102*, 15213–15218.

Fukuyama, M., Rougvie, A.E., and Rothman, J.H. (2006). C. elegans DAF-18/PTEN mediates nutrient-dependent arrest of cell cycle and growth in the germline. Curr. Biol. *16*, 773–779.

Fu, L., Pelicano, H., Liu, J., Huang, P., and Lee, C. (2002). The circadian gene Period2 plays an important role in tumor suppression and DNA damage response in vivo. Cell *111*, 41–50.

Gaddameedhi, S., Selby, C.P., Kaufmann, W.K., Smart, R.C., and Sancar, A. (2011). Control of skin cancer by the circadian rhythm. Proc. Natl. Acad. Sci. USA *108*, 18790–18795.

Geyfman, M., Kumar, V., Liu, Q., Ruiz, R., Gordon, W., Espitia, F., Cam, E., Millar, S.E., Smyth, P., Ihler, A., et al. (2012). Brain and muscle Arnt-like protein-1 (BMAL1) controls circadian cell proliferation and susceptibility to UVB-induced DNA damage in the epidermis. Proc. Natl. Acad. Sci. USA *109*, 11758–11763.

Groszer, M., Erickson, R., Scripture-Adams, D.D., Dougherty, J.D., Le Belle, J., Zack, J.A., Geschwind, D.H., Liu, X., Kornblum, H.I., and Wu, H. (2006). PTEN negatively regulates neural stem cell self-renewal by modulating G0-G1 cell cycle entry. Proc. Natl. Acad. Sci. USA *103*, 111–116.

Guldberg, P., thor Straten, P., Birck, A., Ahrenkiel, V., Kirkin, A.F., and Zeuthen, J. (1997). Disruption of the MMAC1/PTEN gene by deletion or mutation is a frequent event in malignant melanoma. Cancer Res. *57*, 3660–3663.

He, X.C., Yin, T., Grindley, J.C., Tian, Q., Sato, T., Tao, W.A., Dirisina, R., Porter-Westpfahl, K.S., Hembree, M., Johnson, T., et al. (2007). PTEN-deficient intestinal stem cells initiate intestinal polyposis. Nat. Genet. *39*, 189–198.

Hobert, J.A., and Eng, C. (2009). PTEN hamartoma tumor syndrome: an overview. Genet. Med. *11*, 687–694.

Hoogerwerf, W.A., Shahinian, V.B., Cornélissen, G., Halberg, F., Bostwick, J., Timm, J., Bartell, P.A., and Cassone, V.M. (2010). Rhythmic changes in colonic motility are regulated by period genes. Am. J. Physiol. Gastrointest. Liver Physiol. *298*, G143–G150.

Horsley, V., Aliprantis, A.O., Polak, L., Glimcher, L.H., and Fuchs, E. (2008). NFATc1 balances quiescence and proliferation of skin stem cells. Cell *132*, 299–310.

Itahana, K., Zou, Y., Itahana, Y., Martinez, J.L., Beausejour, C., Jacobs, J.J.L., Van Lohuizen, M., Band, V., Campisi, J., and Dimri, G.P. (2003). Control of the replicative life span of human

fibroblasts by p16 and the polycomb protein Bmi-1. Mol. Cell. Biol. *23*, 389–401.

Ito, M., Yang, Z., Andl, T., Cui, C., Kim, N., Millar, S.E., and Cotsarelis, G. (2007). Wnt-dependent de novo hair follicle regeneration in adult mouse skin after wounding. Nature *447*, 316–320.

Jacobs, J.J., Kieboom, K., Marino, S., DePinho, R.A., and van Lohuizen, M. (1999a). The oncogene and Polycomb-group gene bmi-1 regulates cell proliferation and senescence through the ink4a locus. Nature *397*, 164–168.

Jacobs, J.J., Scheijen, B., Voncken, J.W., Kieboom, K., Berns, A., and van Lohuizen, M. (1999b). Bmi-1 collaborates with c-Myc in tumorigenesis by inhibiting c-Myc-induced apoptosis via INK4a/ARF. Genes Dev. *13*, 2678–2690.

Jaks, V., Kasper, M., and Toftgård, R. (2010). The hair follicle—a stem cell zoo. Exp. Cell Res. *316*, 1422–1428.

Janich, P., Pascual, G., Merlos-Suárez, A., Batlle, E., Ripperger, J., Albrecht, U., Cheng, H.Y.M., Obrietan, K., Di Croce, L., and Benitah, S.A. (2011). The circadian molecular clock creates epidermal stem cell heterogeneity. Nature *480*, 209–214.

Kalaany, N.Y., and Sabatini, D.M. (2009). Tumours with PI3K activation are resistant to dietary restriction. Nature *458*, 725–731.

Kamijo, T., Zindy, F., Roussel, M.F., Quelle, D.E., Downing, J.R., Ashmun, R.A., Grosveld, G., and Sherr, C.J. (1997). Tumor suppression at the mouse INK4a locus mediated by the alternative reading frame product p19ARF. Cell *91*, 649–659.

Kobielak, K., Pasolli, H.A., Alonso, L., Polak, L., and Fuchs, E. (2003). Defining BMP functions in the hair follicle by conditional ablation of BMP receptor IA. J. Cell Biol. *163*, 609–623.

Kobielak, K., Stokes, N., de la Cruz, J., Polak, L., and Fuchs, E. (2007). Loss of a quiescent niche but not follicle stem cells in the absence of bone morphogenetic protein signaling. Proc. Natl. Acad. Sci. USA *104*, 10063–10068.

Korkaya, H., Paulson, A., Charafe-Jauffret, E., Ginestier, C., Brown, M., Dutcher, J., Clouthier, S.G., and Wicha, M.S. (2009). Regulation of mammary stem/progenitor cells by PTEN/Akt/beta-catenin signaling. PLoS Biol. *7*, e1000121.

Langton, A.K., Herrick, S.E., and Headon, D.J. (2008). An extended epidermal response heals cutaneous wounds in the absence of a hair follicle stem cell contribution. J. Invest. Dermatol. *128*, 1311–1318.

Lavker, R.M., Sun, T.T., Oshima, H., Barrandon, Y., Akiyama, M., Ferraris, C., Chevalier, G., Favier, B., Jahoda, C.A.B., Dhouailly, D., et al. (2003). Hair follicle stem cells. J. Investig. Dermatol. Symp. Proc. *8*, 28–38.

Lee, J.Y., Nakada, D., Yilmaz, O.H., Tothova, Z., Joseph, N.M., Lim, M.S., Gilliland, D.G., and Morrison, S.J. (2010). mTOR activation induces tumor suppressors that inhibit leukemogenesis and deplete hematopoietic stem cells after Pten deletion. Cell Stem Cell *7*, 593–605.

Lessard, J., and Sauvageau, G. (2003). Bmi-1 determines the proliferative capacity of normal and leukaemic stem cells. Nature *423*, 255–260.

Li, G., Robinson, G.W., Lesche, R., Martinez-Diaz, H., Jiang, Z., Rozengurt, N., Wagner, K.U., Wu, D.C., Lane, T.F., Liu, X., et al. (2002). Conditional loss of PTEN leads to precocious development and neoplasia in the mammary gland. Development *129*, 4159–4170.

Liu, H., Fergusson, M.M., Castilho, R.M., Liu, J., Cao, L., Chen, J., Malide, D., Rovira, I.I., Schimel, D., Kuo, C.J., et al. (2007). Augmented Wnt signaling in a mammalian model of accelerated aging. Science *317*, 803–806.

Lin, K.K., Kumar, V., Geyfman, M., Chudova, D., Ihler, A.T., Smyth, P., Paus, R., Takahashi, J.S., and Andersen, B. (2009). Circadian clock genes contribute to the regulation of hair follicle cycling. PLoS Genet. *5*, e1000573.

Liu, J., Cao, L., Chen, J., Song, S., Lee, I.H., Quijano, C., Liu, H., Keyvanfar, K., Chen, H., Cao, L.Y., et al. (2009). Bmi1 regulates mitochondrial function and the DNA damage response pathway. Nature *459*, 387–392.

Matsumoto, C.S., Almeida, L.O., Guimarães, D.M., Martins, M.D., Papagerakis, P., Papagerakis, S., Leopoldino, A.M., Castilho, R.M., and Squarize, C.H. (2017). PI3K-PTEN dysregulation leads to mTOR-driven upregulation of the core clock gene BMAL1 in normal and malignant epithelial cells. Oncotarget *7*, 42393–42407.

Mascré, G., Dekoninck, S., Drogat, B., Youssef, K.K., Broheé, S., Sotiropoulou, P.A., Simons, B.D., and Blanpain, C. (2012). Distinct contribution of stem and progenitor cells to epidermal maintenance. Nature *489*, 257–262.

Merrill, B.J., Gat, U., DasGupta, R., and Fuchs, E. (2001). Tcf3 and Lef1 regulate lineage differentiation of multipotent stem cells in skin. Genes Dev. *15*, 1688–1705.

Ming, M., Feng, L., Shea, C.R., Soltani, K., Zhao, B., Han, W., Smart, R.C., Trempus, C.S., and He, Y.Y. (2011). PTEN positively regulates UVB-induced DNA damage repair. Cancer Res. *71*, 5287–5295.

Mitra, S. (2011). Does evening sun increase the risk of skin cancer? Proc. Natl. Acad. Sci. USA *108*, 18857–18858.

Mohrin, M., Bourke, E., Alexander, D., Warr, M.R., Barry-Holson, K., Le Beau, M.M., Morrison, C.G., and Passegué, E. (2010). Hematopoietic stem cell quiescence promotes error-prone DNA repair and mutagenesis. Cell Stem Cell *7*, 174–185.

Morris, R.J., Liu, Y., Marles, L., Yang, Z., Trempus, C., Li, S., Lin, J.S., Sawicki, J.A., and Cotsarelis, G. (2004). Capturing and profiling adult hair follicle stem cells. Nat. Biotechnol. *22*, 411–417.

Müller-Röver, S., Handjiski, B., van der Veen, C., Eichmüller, S., Foitzik, K., McKay, I.A., Stenn, K.S., and Paus, R. (2001). A comprehensive guide for the accurate classification of murine hair follicles in distinct hair cycle stages. J. Invest. Dermatol. *117*, 3–15.

Nardella, C., Clohessy, J.G., Alimonti, A., and Pandolfi, P.P. (2011). Pro-senescence therapy for cancer treatment. Nat. Rev. Cancer *11*, 503–511.

Nowak, J.A., Polak, L., Pasolli, H.A., and Fuchs, E. (2008). Hair follicle stem cells are specified and function in early skin morphogenesis. Cell Stem Cell *3*, 33–43.

Park, I.K., Morrison, S.J., and Clarke, M.F. (2004). Bmi1, stem cells, and senescence regulation. J. Clin. Invest. *113*, 175–179.

Paus, R., and Foitzik, K. (2004). In search of the "hair cycle clock": a guided tour. Differentiation *72*, 489–511.

Paus, R., Müller-Röver, S., and Botchkarev, V.A. (1999a). Chronobiology of the hair follicle: hunting the "hair cycle clock". J. Investig. Dermatol. Symp. Proc. *4*, 338–345.

Paus, R., Müller-Röver, S., Van Der Veen, C., Maurer, M., Eichmüller, S., Ling, G., Hofmann, U., Foitzik, K., Mecklenburg, L., and Handjiski, B. (1999b). A comprehensive guide for the recognition and classification of distinct stages of hair follicle morphogenesis. J. Invest. Dermatol. *113*, 523–532.

Pietras, E.M., Warr, M.R., and Passegué, E. (2011). Cell cycle regulation in hematopoietic stem cells. J. Cell Biol. *195*, 709–720.

Plikus, M.V., Mayer, J.A., de la Cruz, D., Baker, R.E., Maini, P.K., Maxson, R., and Chuong, C.M. (2008). Cyclic dermal BMP signalling regulates stem cell activation during hair regeneration. Nature *451*, 340–344.

Plikus, M.V., Vollmers, C., de la Cruz, D., Chaix, A., Ramos, R., Panda, S., and Chuong, C.M. (2013). Local circadian clock gates cell cycle progression of transient amplifying cells during regenerative hair cycling. Proc. Natl. Acad. Sci. USA *110*, E2106–E2115.

Polak, R., and Buitenhuis, M. (2012). The PI3K/PKB signaling module as key regulator of hematopoiesis: implications for therapeutic strategies in leukemia. Blood *119*, 911–923.

Sanders, D.S.A., and Carr, R.A. (2007). The use of immunohistochemistry in the differential diagnosis of common epithelial tumours of the skin. Curr. Diagn. Pathol. *13*, 237–251.

Segrelles, C., García-Escudero, R., Garín, M.I., Aranda, J.F., Hernández, P., Ariza, J.M., Santos, M., Paramio, J.M., and Lorz, C. (2014). Akt signaling leads to stem cell activation and promotes tumor development in epidermis. Stem Cells *32*, 1917–1928.

Serrano, M., Lee, H., Chin, L., Cordon-Cardo, C., Beach, D., and DePinho, R.A. (1996). Role of the INK4a locus in tumor suppression and cell mortality. Cell *85*, 27–37.

Sherr, C.J. (2004). Principles of tumor suppression. Cell *116*, 235–246.

Squarize, C.H., Castilho, R.M., and Gutkind, J.S. (2008). Chemoprevention and treatment of experimental Cowden's disease by mTOR inhibition with rapamycin. Cancer Res. *68*, 7066–7072.

Squarize, C.H., Castilho, R.M., Bugge, T.H., and Gutkind, J.S. (2010). Accelerated wound healing by mTOR activation in genetically defined mouse models. PLoS One *5*, e10643.

Squarize, C.H., Castilho, R.M., Abrahao, A.C., Molinolo, A., Lingen, M.W., and Gutkind, J.S. (2013). PTEN deficiency contributes to the development and progression of head and neck cancer. Neoplasia *15*, 461–471.

Sun, H., Lesche, R., Li, D.M., Liliental, J., Zhang, H., Gao, J., Gavrilova, N., Mueller, B., Liu, X., and Wu, H. (1999). PTEN modulates cell cycle progression and cell survival by regulating phosphatidylinositol 3,4,5,-trisphosphate and Akt/protein kinase B signaling pathway. Proc. Natl. Acad. Sci. USA *96*, 6199–6204.

Suzuki, A., Itami, S., Ohishi, M., Hamada, K., Inoue, T., Komazawa, N., Senoo, H., Sasaki, T., Takeda, J., Manabe, M., et al. (2003). Keratinocyte-specific Pten deficiency results in epidermal hyperplasia, accelerated hair follicle morphogenesis and tumor formation. Cancer Res. *63*, 674–681.

Tanioka, M., Yamada, H., Doi, M., Bando, H., Yamaguchi, Y., Nishigori, C., and Okamura, H. (2009). Molecular clocks in mouse skin. J. Invest. Dermatol. *129*, 1225–1231.

Trempus, C.S., Morris, R.J., Bortner, C.D., Cotsarelis, G., Faircloth, R.S., Reece, J.M., and Tennant, R.W. (2003). Enrichment for living murine keratinocytes from the hair follicle bulge with the cell surface marker CD34. J. Invest. Dermatol. *120*, 501–511.

White, A.C., Khuu, J.K., Dang, C.Y., Hu, J., Tran, K.V., Liu, A., Gomez, S., Zhang, Z., Yi, R., Scumpia, P., et al. (2014). Stem cell quiescence acts as a tumour suppressor in squamous tumours. Nat. Cell Biol. *16*, 99–107.

Yan, H., Dobbie, Z., Gruber, S.B., Markowitz, S., Romans, K., Giardiello, F.M., Kinzler, K.W., and Vogelstein, B. (2002). Small changes in expression affect predisposition to tumorigenesis. Nat. Genet. *30*, 25–26.

Yilmaz, O.H., Valdez, R., Theisen, B.K., Guo, W., Ferguson, D.O., Wu, H., and Morrison, S.J. (2006). Pten dependence distinguishes haematopoietic stem cells from leukaemia-initiating cells. Nature *441*, 475–482.

Zhang, J., Grindley, J.C., Yin, T., Jayasinghe, S., He, X.C., Ross, J.T., Haug, J.S., Rupp, D., Porter-Westpfahl, K.S., Wiedemann, L.M., et al. (2006). PTEN maintains haematopoietic stem cells and acts in lineage choice and leukaemia prevention. Nature *441*, 518–522.

Zhang, D., Tong, X., Arthurs, B., Guha, A., Rui, L., Kamath, A., Inoki, K., and Yin, L. (2014). Liver clock protein BMAL1 promotes de novo lipogenesis through insulin-mTORC2-AKT signaling. J. Biol. Chem. *289*, 25925–25935.

Stem Cell Reports, Volume *9*

Supplemental Information

PTEN Mediates Activation of Core Clock Protein BMAL1 and Accumulation of Epidermal Stem Cells

Chiara Zagni, Luciana O. Almeida, Tarek Balan, Marco T. Martins, Luciana K. Rosselli-Murai, Petros Papagerakis, Rogerio M. Castilho, and Cristiane H. Squarize

Supplementary Data

PTEN mediates activation of core clock protein BMAL1 and accumulation of epidermal stem cells

Chiara Zagni1, §, Luciana O. Almeida[1], §, Tarek Balan[3], Marco T. Martins[1], Luciana K. Rosselli-Murai[1], Petros Papagerakis[3, 4], Rogerio M. Castilho[1,2], and Cristiane H. Squarize[1,2,*]

Supplementary Figure Legends

Figure S1 related to Figure 1. **PTEN ablation in the epidermis leads to altered hair cycle hair and enlarged ORS. A.** Representative H&E sections of the first and second synchronous hair cycle showing the histological changes of the hair follicles during each phase at the indicated time points or age (n=5 mice per group). Note the prolonged growth of hair follicles at anagen (control p7-p14), followed by involution of the hair follicles (catagen) at P17 and the small HFs during the resting phase (telogen) at P21 and P24, during the first hair cycle in control, K14Cre-Pten$^{F/+}$ and K14Cre-Pten$^{F/F}$ mice. The second hair cycle phase is normal in control mice. K14Cre-Pten$^{F/+}$ mice display prolonged hair follicles (anagen) as seen in p26 to p34, followed by catagen and telogen. K14Cre-Pten$^{F/F}$ mice show prolonged resting period displaying short HF (telogen) as seen in p21 to p34. Scale bars: 200 μm **B**. Examples of interfollicular epithelium showing increasing on the terminal differentiation marker fillagrin in the upper most layers of epidermis, CK10 in the spinour layer, and CK14 at basal layer in the follicular epithelium of PTEN deficient mice. Scale bars: 50 μm. **C**. In the hair follicle, all phenotypes

displayed similar CK10. Scale bars: 50 μm **D.** Increased expression of CK6 indicated an enlarged outer root sheet (ORS) in PTEN deficient mice**.** Scale bars: 50 μm **E.** B-catenin staining (Scale bars: 25 μm) and **(F)** pSMAD expression were not different among phonotypes (mean percentage ± S.E.M, data from 3 independent experiments).

Figure S2 related to Figure 2: **PTEN homozygous deletion resulted in quiescence and delayed hair re-grow. A**. Representative pictures of hair regrowth after shaving in control, K14Cre-Pten$^{F/+}$, and K14Cre-Pten$^{\mathbf{F/F}}$ mice. Note that control mice completely recover dorsal hair coats by day 30 after shaving. K14Cre-Pten$^{\mathbf{F/+}}$ mice have delayed regrowth of hair coats compared to littermate controls. K14Cre-Pten$^{\mathbf{F/F}}$ mice fail to regrow hair coats even at 60 days after shaving. **B.** Graphic representation of hair shaft measurements after shaving. The data are represented as a mean ± S.E.M (n=9 mice per genotype; *P*-value is illustrated as ns $p>0.05$; *$p<0.05$, **$p<0.01$ and ***$p<0.001$).

Figure S3 related to figure 3. **PER2 ablation leads to Bmal1 activation and increase numbers of stem cells. A.** Similar to what we observe in HF, Bmal1 is overexpressed in the interfollicular component of the epidermis of K14Cre-PtenF/+ and K14Cre-PtenF/F mice compared to control mice, as seen on the quantitative graphic (P-value is illustrated as * $p<0.05$; ** $p<0.01$, ***$p<0.001$). **B**. Immunoblot analysis of human keratinocyte (NOK-SI) cells transfected with siRNA Control and siRNA for PTEN. Immunoblot analysis and of human keratinocyte (NOK-SI) cells transfected with siRNA Control and siRNA for *PTEN*. PTEN knockdown is achieved with 10 nM siRNA concentrations. GAPDH was used as a loading control. **C**. Graphic representation of PTEN-deficient cells with increased phosphorylation AKT (pAKTSer473) (mean ± S.E.M, data from triplicates) **D.** m*Per2* knockout mice have accumulation of nuclear BMAL1 protein in the

interfollicular and follicular epidermis. Bar graph reveals a statistically significant accumulation of nuclear BMAL1 in the interfollicular and follicular epidermis of mPer2 knockout mice compared to age-matched controls. **E.** Flow cytometric analysis of epithelial cells shows stem cells isolated from control and m*Per2* KO mice. Graphic shows accumulation of $CD34^{+}\alpha6^{+}$ cells in mPer2 KO mice compared to control mice. (mean percentage ± S.E.M, n=4 fields per 3 mice per genotype (A&D); $n=10^{4}$ cells per genotype (E), *P*-value is illustrated as *** $p<0.001$).

Figure S4 related to Figure 4**. Loss of PTEN triggers activation of epidermal senescence characterized by the expression of $p16^{ink4}$ and depletion of BMI-1. A.** Whole-mount specimen from the skin (tail) displaying HFs stained with Hoechst 33342 (blue) and the γ-H2AX senescence marker (red). Samples from K14Cre-$Pten^{F/+}$ mice show moderate accumulation of γ-H2AX staining in the HF bulge compared to high levels observed in K14Cre-$Pten^{F/F}$ mice. Scale bars: 25 μm. **B.** Presence of epidermal senescence in the skin of K14Cre-$Pten^{F/F}$ mice. The senescence-associated β-Galactosidase assay produces SA-β-Gal staining (blue) in the follicular and interfollicular epidermal areas in K14Cre-/$Pten^{F/F}$ mice. Scale bars: 30 μm **C.** Immunoblot of mouse skin confirms reduced protein levels of PTEN in K14Cre-$Pten^{F/+}$ and PTEN ablation in K14Cre-$Pten^{F/F}$ mice compared to control littermates (lysates from pooled cells isolated from 3 mice per genotype). Note that upon deletion of PTEN, BMI-1 is progressively downregulated until it is completely absent in tumor cells. This effect is accompanied by increased $P16^{Ink4}$ levels exclusively in tumor samples. GAPDH - loading control.

Supplementary Experimental Procedures

Experimental mice / In vivo experiments

Animals received food, standard rodent chow, and water ad libitum and soft diet supplement as needed in compliance with AAALAC guidelines. Animals were observed daily by the investigators and animal care staff. Any animals displaying signs of discomfort, wasting, or other signs indicative of distress were treated appropriately to alleviate discomfort or euthanized following the procedures described in the approved protocol. *Pten* knockout mice were crossed to generate K14Cre $Pten^{F/+}$ mice; K14Cre $Pten^{F/+}$ mice following by backcross with $Pten^{F/F}$ mice to generate litters of K14Cre $Pten^{F/F}$, K14Cre $Pten^{F/+}$, and control mice. Genotyping was performed on Pten floxed mice using primers P1 (5'-ACTCAAGGCAGGGA TGAGC-3') and P2 (5'-GCCCCGATGCAATAAATATG-3') and on K14Cre mice using primers P3 (5'-CACGATACACCTGACTAGCTGGGTG-3') and P4 (5'-CATCACCCACAGGCTAGCGCCAACT-3') as described (Squarize et al., 2008).

mPer2 knockout mice (Per2tm1Drw) were genotyped using primers xj11 (5′-AGAACTTGTTGCTCCTGCTT-3′) and xj8 (5′-GGAAGCTTGTAAGGGGTGGT-3′) (Bae et al., 2001). Where indicated, Ad-shLacZ control or Ad-shBmal1 shRNA adenoviruses were injected into day 3 mice subcutaneous injections at the dose of 1×10^{12} plaque-forming units. (Zhang et al, 2014, Liu et al, 2007). When indicated, mice were treated with 4NQO (50 μg/ml) or vehicle in drinking water and followed for 21 weeks (Squarize et al., 2013). LRC was performed by injecting mice with BrDU 50 μg/g of body weight) as described (Bickenbach and Chism, 1998)(Braun and Watt, 2004). Specifically, mice were injected intraperitoneally with 50 ug/g two times per day for 3

days (label retention period) and analyzed 28 days later after last injection. Skin was isolated and processed for FACS analyses.

Isolation of the hair follicle stem cells, FACS analysis, and qPCR

Littermate mice were used for these experiments as previously described (Castilho et al., 2009). Briefly, the subcutis underlying the dorsal skin was removed, and the epithelial cell layer was trypsinized for 2 hours at 37°C. Epithelial cell suspensions were filtered through 70 μm mesh filters (BD Bioscience) to achieve a single cell suspension. Cells were incubated with 2% FBS in PBS on ice for 30 minutes, followed by addition of the primary antibody (CD34 - BD Pharmingen, CD49f - BD Pharmingen) coupled with FITC (BD Pharmingen) and PE/Cye5 (BD Pharmingen). The cDNA synthesis and qPCR were performed in HFSC after FACS-sorting using Applied Biosystems reagents and kits following manufacture's instructions. TaqMan Gene Expression Assays (Applied Biosystems) were used for Bmal1 (Arntl, Mm00500226_m1) and ACTB (Control, Mm00607939_s1). Three measurement replicates were performed, and the value of each cDNA was calculated using the ΔCt method and normalized to the value of the housekeeping gene control. The data were plotted as -fold change. For cell cycle analysis, cells were permeabilized with Triton X-100 (0.1%) and propidium iodide (50 μg/ml) was added for nuclear staining. qPCR assays were conducted at the Molecular Cell Biology Core at the UM School of Dentistry. FACS experiments were performed at the Flow Cytometry Core at the University of Michigan.

Histological sections and Shaving assay

The dorsal skin of mice was shaved and monitored for up to 70 days or until the hair coat

regrew. Hair regrowth was monitored weekly. Skin samples were fixed overnight in 4% PFA and transferred to 70% ethanol before processing. Hematoxylin and eosin (H&E) staining was performed on formalin-fixed and paraffin-embedded serial sections according to standard procedures. Periodic Acid-Schiff staining (PAS kit, Sigma-Aldrich) was performed as described by the manufacturer.

Cell lineage and reagents

HN13, NIH3T3 and NOK-SI cells (Castilho et al., 2010) were cultured in DMEM supplemented with 10% fetal bovine serum, 100 units/ml penicillin, 100 μg/ml streptomycin, and 250 ng/ml amphotericin B. Cells were maintained in a 5% CO2-humidified incubator at 37^0C. IHC and IF was performed on PFA or and frozen tissue sections. IHC or IF was performed using anti-CD34 (eBiosciences, 13-0341), gamma-H2AX (EMD Millipore, 05-636), K15 (Abcam, ab80522), K10 (BioLegend, PRB-159P), K14 (BioLegend, PRB-155P), K6 (Abcam, ab18586), Beta-Catenin (BD 610153), p-SMAD (Cell Signaling Technology, 9511), and BMAL1 (Novus Bioscience, NB100-2288) O/N at 4^oC. Where indicated, animals were euthanized at the same time point. Briefly, after antigen retrieval using 10 mM sodium citrate buffer, tissues were treated with 6% H_2O_2 and then 3% BSA for 1 hr. Cells were incubated with primary antibody O/N at 4^oC. BMAL1 were analyzed on tissue collected at 8 pm. IHC reactions were developed with 3,3-diaminobenzidine (DAB, Sigma-Aldrich), and IF reactions were conjugated with TRITC and FITC secondary antibodies and stained with Hoechst 33342 (Invitrogen) for visualization of DNA content. Images were taken using a QImaging ExiAqua monochrome digital camera attached to a Nikon Eclipse 80i Microscope (Nikon, Melville, NY) and visualized with QCapturePro software.

PTEN siRNA knockdown, plasmids, and adenoviruses

Knockdown of PTEN was performed in NOK-SI and HN13 cells using siRNA as previously described (Squarize et al., 2006). Briefly, cells were seeded in 24-well plates and transfected with 12.5 nM double-stranded RNA oligonucleotides directed against human *PTEN* (NM_000314; forward: 5′- CCA AUG GCU AAG UGA AGA UGA CAA U [dT] [dT]-3′ and reverse: 5′- AUU GUC AUC UUC ACU UAG CCA UUG G [dT] [dT] -3′) (Invitrogen). Optimal concentrations and time points were determined by dilution curves of siRNA for each target and immunoblot analyses. The sequences of the control negative siRNA (Invitrogen) oligonucleotides were as follows: 5′-UUC UCC GAA CGU GUC ACG UdTdT-3′ and 5′-ACG UGA CAC GUU CGG AGA AdTdT-3′. Circadian cycle was analyzed after cells were synchronized with 10μM of Forkoslin for 2 hours. NIH3T3 cells stable cells lines were produced with pC3.1myr-AKT or control plasmid. Ad-shBmal1 shRNA or Ad-shLacZ control adenoviruses were used to transduce cells. All assays were run in triplicates or sextuplicates depending on the experiment. For invivo assay, refer to experimental model. As previously described, ShRNA were generated by Dr. Yin lab (Zhang et al., 2014).

Preparation of whole mount and SA-β-Galactosidase detection

Epidermal whole mounts were prepared by separating the epidermis from the underlying dermis as an intact sheet using dispase. The epidermis was fixed in 4% paraformaldehyde and stained with primary and secondary antibodies. Whole mounts were counterstained with Hoechst 33342. Images were taken using a QImaging ExiaAqua monochrome digital camera attached to a Nikon Eclipse 80i Microscope (Nikon, Melville, NY) and visualized with QCapturePro software. Images are x20 magnification unless otherwise

indicated. The senescence-associated Beta-Galactosidase (SA-β-Gal) detection kit was used (Roche) at pH 6.0 as described by the manufacturer.

Immunoblot

Single cell suspensions were obtained from mouse epidermis as described in the FACS section of the Materials and Methods or from NOK-SI cells. Cells were lysed (0.2 M Tris pH 7.5, SDS 20%, 14.3 M 2-betamercaptoetanol), and 30 μg of protein was resolved by SDS–polyacrylamide gel electrophoresis. Immunoblotting was performed using standard techniques. The membranes were blocked for 1h at room temperature with 5% milk and incubated with PTEN (Cell Signaling Technology, 9559), AKT (Cell Signaling Technology, 4691), p-AKT (Cell Signaling Technology 4060), BMAL1 (Novus Biologicals, NB100-2288), BMI-1 (Cell Signaling Technology, 5856), p16 (BD Pharmingen, 551153), and GAPDH (EMD Millipore, CB1001) primary antibodies. Membranes were then incubated with the IgG-HRP conjugated secondary antibody, and immunoblots were developed using a chemiluminescent-HRP substrate.

Statistical Analysis

Statistical analysis of bulge size, BMAL1 positive cells and gamma-H2AX stain and others were performed by one-way analysis of variance (ANOVA) followed by Tukey's multiple comparison tests. Hair growth and other analyses were assessed by two-way ANOVA followed by the Bonferroni posttest. All statistical analysis was performed using GraphPad Prism (GraphPad Software, San Diego, CA). Asterisks denote statistical significance (ns-$p>0.05$; * $p<0.05$; ** $p<0.01$; and *** $p<0.001$).

Supplementary References

Bickenbach, J.R., Chism, E., 1998. Selection and extended growth of murine epidermal stem cells in culture. Exp. Cell Res. 244, 184–195.

Braun, K.M., Watt, F.M., 2004. Epidermal label-retaining cells: background and recent applications. J. Investig. Dermatol. Symp. Proc. 9, 196–201. Klaude, M., Eriksson, S., Nygren, J., and Ahnström, G. (1996). The comet assay: mechanisms and technical considerations. Mutat. Res. *363*, 89–96.

Liu H, Fergusson MM, Castilho RM, Liu J, Cao L, Chen J, Malide D, Rovira II, Schimel D, Kuo CJ, Gutkind JS, Hwang PM, Finkel T. (2007) Augmented Wnt signaling in a mammalian model of accelerated aging. Science. 317:803-806.

Squarize, C.H., Castilho, R.M., Sriuranpong, V., Pinto, D.S., Jr, and Gutkind, J.S. (2006). Molecular cross-talk between the NFkappaB and STAT3 signaling pathways in head and neck squamous cell carcinoma. Neoplasia *8*, 733–746.

Zhang D, Tong X, Arthurs B, Guha A, Rui L, Kamath A, Inoki K, Yin L. (2014) Liver clock protein BMAL1 promotes de novo lipogenesis through insulin-mTORC2-AKT signaling. J Biol Chem. 289: 25925-25935.

Suppl. Fig. 1

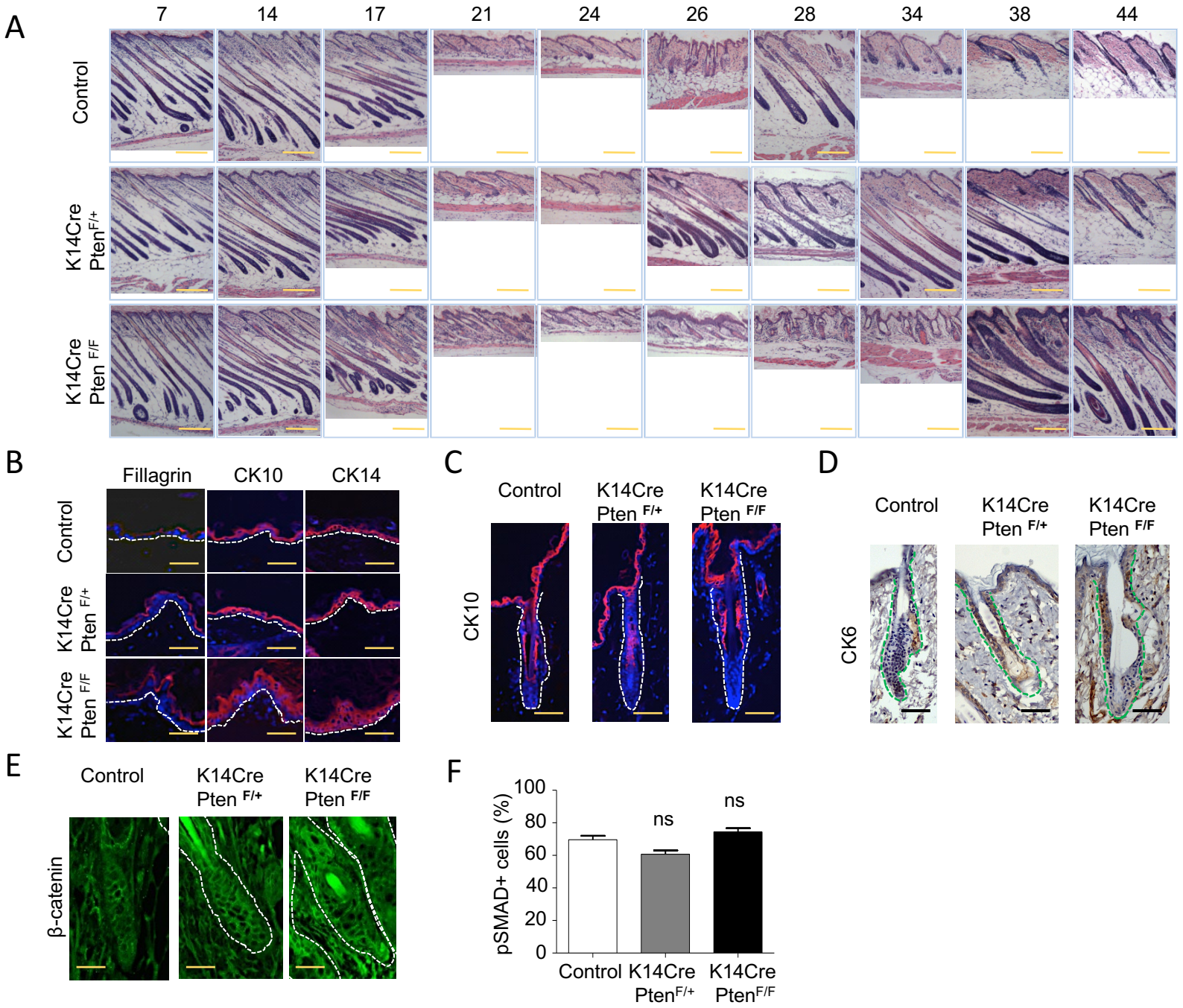
A
7
14
17
21
24
26
28
34
38
44
Control
K14Cre Pten F/+
K14Cre Pten F/F
B
Fillagrin
CK10
CK14
Control
K14Cre Pten F/+
K14Cre Pten F/F
C
Control
K14Cre Pten F/+
K14Cre Pten F/F
CK10
D
Control
K14Cre Pten F/+
K14Cre Pten F/F
CK6
E
Control
K14Cre Pten F/+
K14Cre Pten F/F
β-catenin
F
pSMAD+ cells (%)
100
80
60
40
20
0
ns
ns
Control
K14Cre Pten F/+
K14Cre Pten F/F

Suppl. Fig. 2

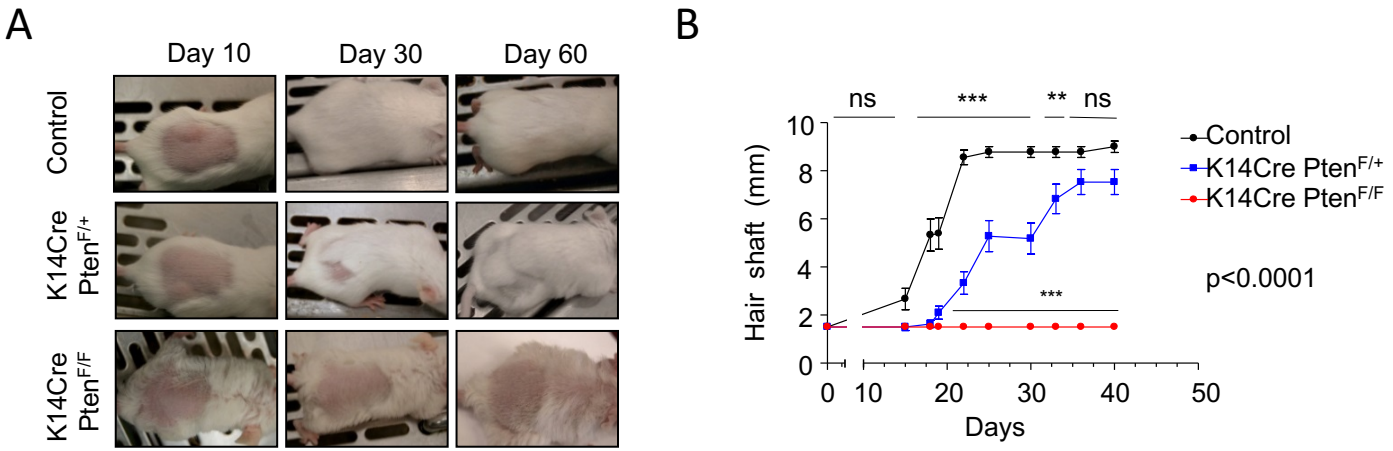
A
Day 10
Day 30
Day 60
Control
K14Cre Pten$^{F/+}$
K14Cre Pten$^{F/F}$
B
ns
***
**
ns
***
Hair shaft (mm)
Days
Control
K14Cre Pten$^{F/+}$
K14Cre Pten$^{F/F}$
p<0.0001

Suppl. Fig. 3

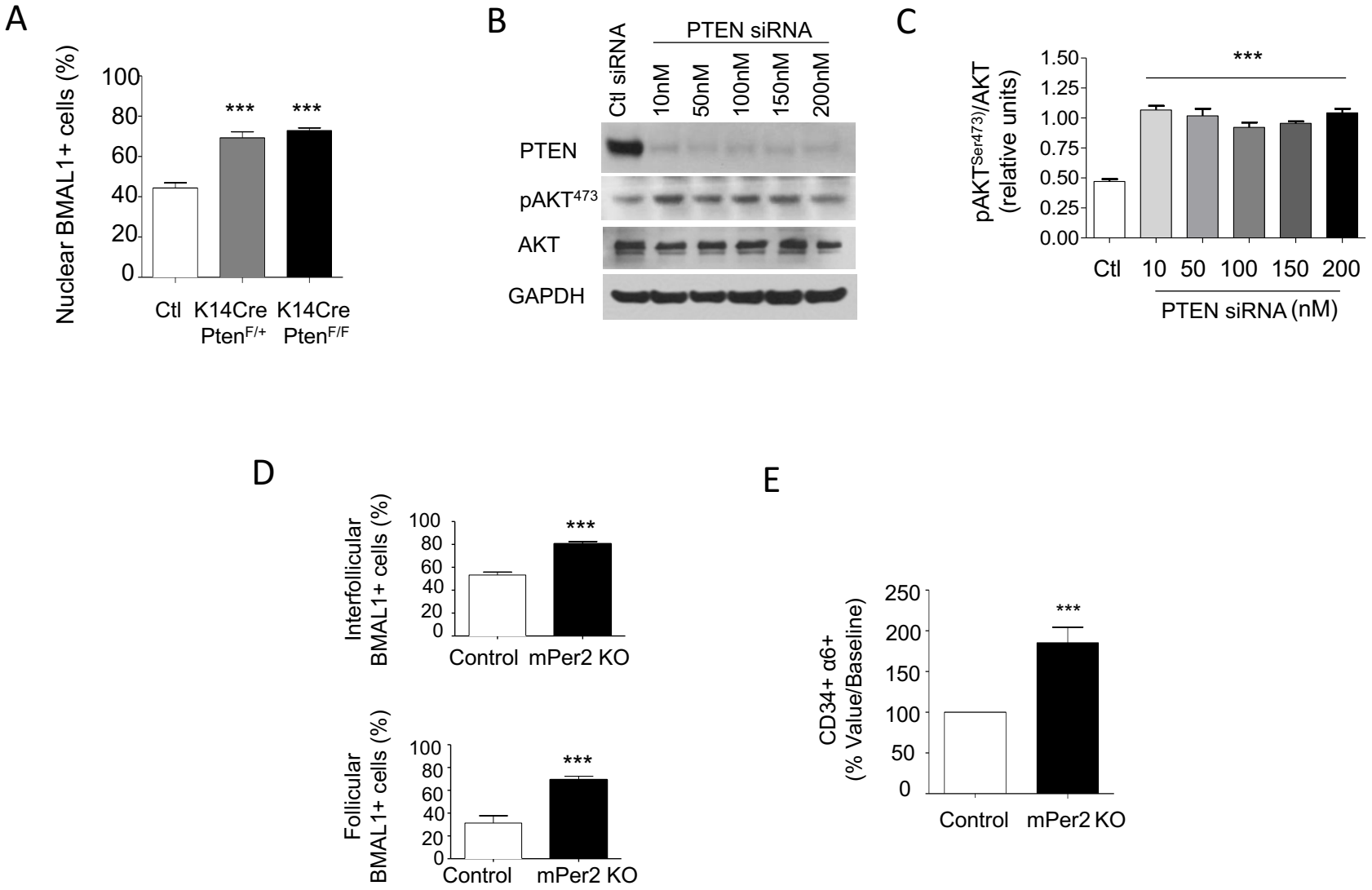
A
Nuclear BMAL1+ cells (%)
100
80
60
40
20
0
***
***
Ctl
K14Cre Pten F/+
K14Cre Pten F/F
B
Ctl siRNA
PTEN siRNA
10nM
50nM
100nM
150nM
200nM
PTEN
pAKT473
AKT
GAPDH
C
pAKTSer473)/AKT (relative units)
1.50
1.25
1.00
0.75
0.50
0.25
0.00
***
Ctl
10
50
100
150
200
PTEN siRNA (nM)
D
Interfollicular BMAL1+ cells (%)
100
80
60
40
20
0
***
Control
mPer2 KO
Follicular BMAL1+ cells (%)
100
80
60
40
20
0
***
Control
mPer2 KO
E
CD34+ α6+ (% Value/Baseline)
250
200
150
100
50
0
***
Control
mPer2 KO

Suppl. Fig. 4

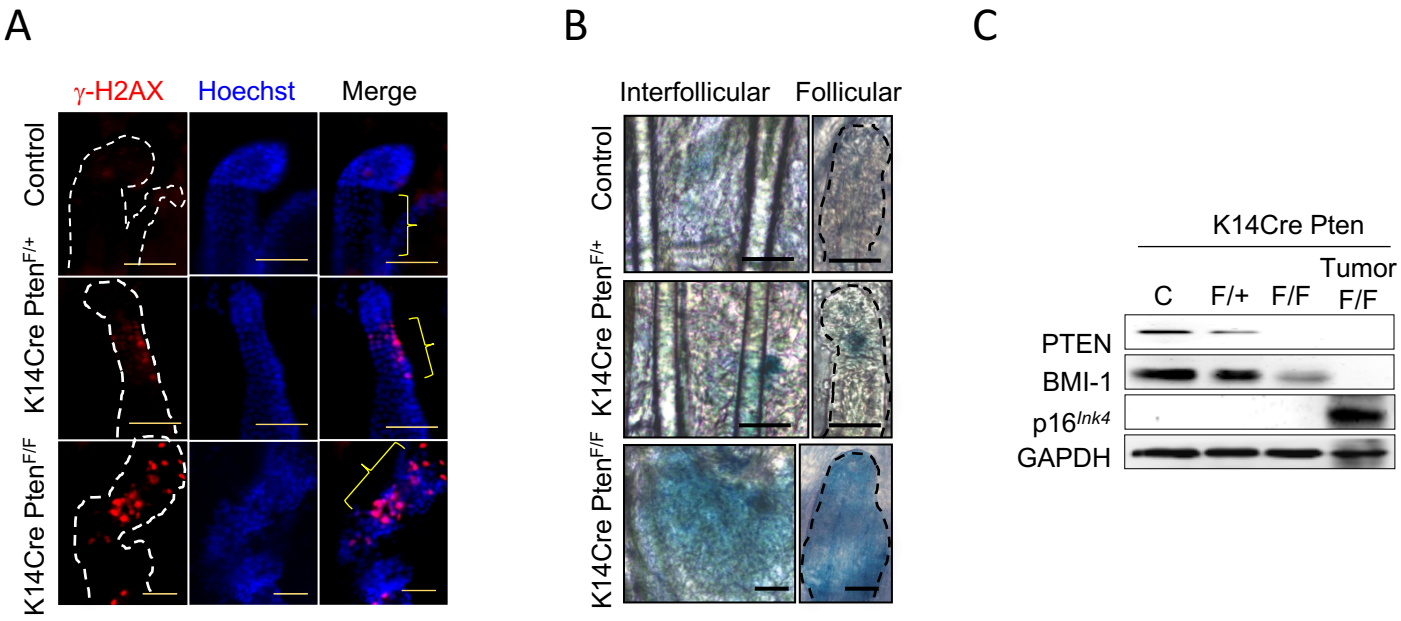
A
γ-H2AX
Hoechst
Merge
Control
K14Cre PtenF/+
K14Cre PtenF/F
B
Interfollicular
Follicular
Control
K14Cre PtenF/+
K14Cre PtenF/F
C
K14Cre Pten
C
F/+
F/F
Tumor F/F
PTEN
BMI-1
p16Ink4
GAPDH